AAEC/E198

AUSTRALIAN ATOMIC ENERGY COMMISSION

RESEARCH ESTABLISHMENT
LUCAS HEIGHTS

RESONANCE PARAMETERS FOR MEASURED keV NEUTRON CAPTURE CROSS SECTIONS

by

A.R. de L. MUSGROVE

May 1969

AUSTRALIAN ATOMIC ENERGY COMMISSION

RESEARCH ESTABLISHMENT

LUCAS HEIGHTS

RESONANCE PARAMETERS FOR MEASURED keV NEUTRON CAPTURE CROSS SECTIONS

by

A. R de L. MUSGROVE

ABSTRACT

All available neutron capture cross sections in the keV region (~ 5 to 100 keV) have been fitted with resonance parameters. Capture cross sections for nuclides with reasonably well known average s-wave parameters but no measured cross section, have been calculated and tabulated using p- and d-wave strength functions interpolated between fitted values. Several of these nuclides are of interest in the theory of slow nucleosynthesis of heavy elements in stars, and the product of cosmic abundance (due to the s-process) and capture cross section at 30 keV has been plotted versus mass number.

CONTENTS

1. INTRODUCTION

An isotropic collision probability programme ICPP has been written for the A.A.E.C. IBM 360/50H computer using methods of calculating collision probabilities described by Doherty (1969a) and a block relaxation scheme for the solution of the multigroup flux equations (Doherty 1969b). This programme can calculate eigenvalues or fixed source problems in slab, spherical or cylindrical geometries, the latter with a number of different boundary conditions.

As the collision probability method offers an alternative to the S_n codes in common use in reactor physics calculations, a survey of some problems was undertaken to determine whether the collision probability method could be considered superior to the S_n methods, in terms of accuracy obtainable per unit computer time. The range of problems is restricted to the isotropic scattering approximation in situations normally solved by one-dimensional transport calculations.

Section 2 is devoted to a problem proposed by Askew (1967), which is a natural uranium graphite cell with annular geometry. The comparison has been extended to more than two groups to obtain a more realistic picture of the calculation which might be undertaken in a serious assessment of this cell. Section 3 discusses the errors involved in the use of the Bonalumi (1961) approximation, which are of interest since the collision probability calculations are competitive in time when this approximation is adequate.

Section 4 is devoted to a fast critical sphere calculation which has been used as a benchmark problem for S_n and collision probability codes. The interesting features of this problem are the slow approach to the correct result by the collision probability method and the flux dip at the centre produced by S_n calculations. The derivation of the spherical collision probability equations is presented in Appendix 1.

Section 5 contains a simple problem in slab geometry which was originally intended to illustrate the difficulties discussed by Meneghetti (1961) but which brought to light another problem involved in the use of S_n methods in slab geometry. As the Meneghetti effect is well known anyway, the discussion has been restricted to the other problem which has been noticed.

Section 6 is a summary of some calculations relating to the outer boundary conditions on a Wigner-Seitz equivalent cylinder. It has been noticed that the specularly reflecting boundary leads to a higher thermal flux in the moderator than exists in the physical situation (Newmarch 1960) and that this problem can be overcome by the use of a white (or isotropically reflecting) boundary condition. In some natural uranium heavy water lattices the main effect of changing the boundary conditions is to alter the fast fission factor of the cell (up to 2% in k_∞). The results presented in this section are intended to provide some insight into the errors involved in this boundary condition. Appendix 2 describes an interpolation scheme based on the Bonalumi (1961) approximation which can be used to perform resonance absorption calculations, with the outer boundary either square or hexagonal.

Finally, Section 7 contains some comments on the applicability of collision probability methods in the problems under discussion.

2. COMPARISONS ON A PROBLEM OF ASKEW

Askew (1967) has considered a lattice cell consisting of a centrally placed rod of natural uranium of radius 1.5 cm surrounded by an annulus of graphite with outer radius 12 cm. The purpose of his investigation was to examine, in two groups, the effect of mesh interval on the calculated value of lattice parameters such as k, and to compare the merits of S_n and collision probabilities on this type of problem. The complete problem specification is contained in Table 1, which has been copied from the original.

Table 2 contains the results of 2-group calculations performed on an IBM 360/50H computer. The WDSN runs were repeated because it was thought that the 2-group cross sections provided by Askew and listed in Table 1 might not be precisely those used in the original calculations where the 2-group data were presumably generated with the WIMS code (Askew et al. 1966). A constant difference of 0.0001 in k_∞ between the Winfrith runs and those contained in Table 2 is probably due to the four figure specification of cross sections since the precision available on both the KDF9 (48 bits) and the IBM 360 (64 bits in double precision) will ensure agreement to at least ten decimal digits. It was not possible to separate, on the IBM 360, the solution time from the dead time (which is mainly input/output). The total time figures for WDSN therefore include both

solution time and input/output time. However, if we compare the increase in time in going from S_4 to S_8 on the same mesh size we find that the increases are 34 seconds and 20 seconds on the KDF9 and IBM 360 respectively. These increases are purely in solution time and hence we infer that the IBM 360 is approximately 1.7 times faster than the KDF9 on this particular problem. (WDSN is compiled on the IBM 360 using level 2 optimisation by the Fortran H compiler. Using level 0 of the Fortran H compiler the execution speeds on the IBM 360 are about the same as those of the Winfrith KDF9).

The collision probability solutions presented in Table 2 were obtained with the programme ICPP. The results labelled 'Bonalumi white boundary' are based on the approximation of Bonalumi (1961), modified by Jonsson (1963) and incorporated in the Winfrith programme PERSEUS (Green 1964). The results labelled 'integration white boundary' are obtained from a numerical integration of the PIJ type (Beardwood et al. 1965) similar to the routine used by Askew in his comparison. In each of the collision probability methods the white boundary condition is achieved by the use of a surface/volume reciprocity result.

The WDSN results in Table 2 are essentially those obtained by Askew except for a fairly constant difference of 0.0001 which has been noted previously. The result regarded as the ultimate in this discussion is the S_{16} calculation with 16 mesh intervals in both the fuel and moderator. The question of computing times is obscured in the WDSN runs by the presence of the input/output time, and the times presented in the Solve column are KDF9 times divided by 1.7 in the S_4 and S_8 cases, and total minus input/output time for the S_{16} cases. The time varies with S number roughly as one would expect, that is, with $n(n+1)$ dependence. The dependence on the number of spatial regions is roughly linear, which is mainly due in this problem to the virtual non-existence of upscatter and to the improvement resulting in the spatial iteration for a group when the variation from mesh point to mesh point is reduced.

The picture presented by the collision probability results is not encouraging. The Bonalumi results, which are the same as those obtained by Askew, do come quite close to the correct result using both 8-mesh intervals and 16-mesh intervals in fuel and moderator and it might be thought at first glance that further refinement of the mesh interval would be of value. However, an examination of the white boundary numerical integration results, to which the Bonalumi results are an approximation, shows that in fact the agreement obtained by the Bonalumi method is a fortuitous cancellation of errors and that further refinement of the mesh can only be expected to produce results poorer than those obtained with 16 mesh points.

The time taken to calculate the collision probability matrices by the Bonalumi approximation is quite satisfactory, ranging roughly as the square of the number of mesh points. The time taken to solve the equations varies as $Am^2 + Bm^3$, where m is the number of mesh points. The method of solution is block relaxation with precomputed inverses and the inversion process is responsible for the presence of the m^3 dependence. This method of solution is not well suited to the solution of 2-group problems with 32 mesh points across the cell. In such problems the number of outer iterations necessary to converge the fission source distribution and the number of group passes in each outer iteration are both small so that the compensation for the extra labour of precomputing the inverses of the spatial matrices is inadequate. This problem is, in fact, the worst type of problem to which the chosen method of solving the flux equations can be subjected. Since a cell calculation would normally be run in more than two energy groups, some similar calculations have been run in more groups, based on the same physical cell but with cross sections generated locally and hence not identical with the WIMS set.

Tables 3, 4, and 5 contain results for 2-, 8- and 16-group calculations on the same physical cell. The precise details of material densities, compositions and temperatures were omitted by Askew from the problem specification so we have used what appear to be reasonable guesses for these quantities. In any case we cannot expect precise agreement in k because the multi-group data for these runs has been generated using the local GYMEA code (Pollard and Robinson, 1969). Comparing the 16-group k values with the 2-group results using the Askew data it can be seen that the two systems are physically similar. The 2-group and 8-group results using local data demonstrate the absolute futility of attempting to perform few-group calculations without an adequate spectrum calculation and condensation procedure. The 2-group data produced with GYMEA are the results of a homogenised calculation in 127 groups with subsequent group condensation over the homogeneous spectrum. The Askew 2-group data are formed by a condensation over a set of few region fluxes, calculated in the Spectrox style (Leslie 1963) with collision probability theory in the fuel and diffusion theory in the moderator. It is intended to provide such a condensation scheme for GYMEA in the immediate future.

If we ignore the gross inaccuracies introduced into the calculation by the poor condensation procedure, and concentrate purely on the WDSN-ICPP comparison for corresponding group structures, it becomes apparent that the collision probability method can only be considered competitive, in accuracy per unit computer time, when the Bonalumi approximation is employed. For example, in the 16-group calculations the collision probability method using the Bonalumi approximation is 4 times faster than WDSN using S_4 for 16 mesh points in fuel and moderator and 10 times faster for 8 mesh points in fuel and moderator. In the 2-group calculations performed by Askew this trend is completely obscured and one is led to the false conclusion that no saving in time can result from the use of collision probability methods on this problem.

In the 2-group calculations, WDSN obtains much more consistent values of k when the mesh size is altered than does ICPP. In the 2-group problem the self-scattering term is large and the solution closely resembles that given by diffusion theory. The consistency of the WDSN results derives from the successful attempt of Askew and Brissenden (1963) to select an ordinate set which would cater for this eventuality. Unfortunately such freedom is not available to the collision probability method, which must rely on increasing the number of mesh intervals to reduce the error caused by the flat flux assumption. However, as the number of groups in the calculation increases, the errors in the collision probability results with few regions are reduced to what may be, for sixteen groups, an acceptable level.

Overall, we are led to the conclusion that the S_n method remains superior for this type of problem. This conclusion is based mainly on the accuracy which could be obtained without the detailed knowledge built up here with several hours of computing time. However if more groups than the largest number chosen here were necessitated, by ^{239}Pu for example, then the speed of the collision probability method with Bonalumi's approximation would make it the logical choice.

3. THE ERROR IN THE BONALUMI APPROXIMATION

The principal error associated with the collision probability method usually arises in the assumption that the flux, and hence the scattering source, is flat across each of the chosen mesh intervals. The simple expedient of increasing the number of mesh intervals is the obvious method of reducing this error, though the computation time can increase dramatically if this is attempted on a problem which already has a large number of mesh points. We noted in the last section that increasing the number of mesh points did not result in increasing accuracy if the Bonalumi approximation was employed. This fact had already been demonstrated by Askew (1967) who ascribed the error to inadequacies in the Bonalumi approximation.

To investigate the exact nature of the error in the Bonalumi approximations, a simple 3-region problem was attempted. Both the cross section and the width of the region 2 annulus were varied because it was not clear whether the problem was geometry dependent or mean-free-path dependent. Table 6 contains the collision probabilities calculated by the Bonalumi approximation and Table 7 contains probabilities calculated by numerical integration and labelled 'exact'. Table 8 contains the self collision probabilities for one cell using different orders of Gauss-Legendre quadrature to justify calling the 16-point results of Table 7 exact.

It can be seen that the Bonalumi approximation remains extremely good over this range of variation in cross section, which is reassuring because such variations could easily arise in a multigroup problem. The worst error is in $P_{2,2}$ when the mesh interval has been reduced to 0.01 and then the error is only 10 per cent of a small number. Though the Bonalumi results cannot be used to converge to an ultimate answer for a problem, they should always give close estimates.

4. A SPHERICAL CALCULATION

The report ANL-7416 (1968) contains a number of benchmark problems in reactor physics, including a 6-group calculation of a small spherical critical experiment (GODIVA). For details of the 6-group cross sections etc. the reader is referred to the original report, which also contains solutions obtained using various transport, collision probability, and Monte Carlo programmes on different computers.

The formulae for the calculation of collision probabilities in spherical geometry are contained in Appendix 1. We have performed calculations using constant mesh intervals across the sphere for 10, 20, 30, and 40 mesh intervals using 16-point Gauss-Legendre integration to obtain the collision probabilities of each spherical shell, and for 50 mesh intervals using 4, 8, 12 and 16 order integration. A summary of the k results for these calculations is contained in Table 9.

It can be seen from the results in Table 9 that the collision probability method consistently underestimates k , though the calculation method is ultimately capable of obtaining as exact an estimate of k as may be required. With the present method of solution and the size of computer available the fifty mesh point result, using order 16 Gauss-Legendre integration in the calculation of collision probabilities, is the best estimate available from this programme. This result is obviously not the ultimate result because the change in eigenvalue from 40 to 50 mesh points is 0.00023. However, it appears that order 16 integration is sufficient because the increase from order 12 to order 16 results in a change of 9×10^{-6} in the 50-mesh point problem and this difference would decrease again if the number of mesh points in the problem were to be further increased.

The reason for the consistent underestimation by the collision probability method is that the flux is assumed flat across each of the spherical shells when the collision probabilities are being calculated. This is obviously untrue of all groups for the system under consideration, as the flux declines steadily from the centre of the system to the free outer boundary. The consequence of the flat flux assumption is an overestimate of the leakage probability for each region and hence an underestimate of k . As each of the mesh intervals is made smaller the error in the flat flux assumption is reduced.

An interesting side-problem in this calculation is the erroneous prediction of the central fluxes in S_n calculations. This error is shared by the collision probability calculation for low order Gauss-Legendre quadrature, though the reasons for the same error are entirely different. Table 10 shows the total fluxes in the first five mesh intervals, normalised to unity in the central region, for a set of collision probability calculations and for an S_{16} calculation using WDSN (Green 1967). Results showing a similar dip in the central region have also been obtained from the DSN code (Carlson et al. 1960). This type of error has been noted by Green (1967) and is related to the radial flux representation common to the S_n codes. An S_n method based on an improved spatial flux representation has been written by Green to cope with this problem, though at the expense of some computation time. The collision probability calculation, once the order of quadrature is high enough to avoid the error in the computation of the collision probabilities (and order 16 is certainly sufficient) does not suffer from this error. For systems which do not have a monotonic spatial variation of flux, as does the one under discussion, the collision probability method may be attractive because it does not have a central dip. The error in the estimate of k resulting from the flux dip is usually negligible so the problem which may need collision probabilities is a central reaction rate calculation.

5. A SIMPLE SLAB PROBLEM

The problem is specified completely in Table 11. The cross sections used are not appropriate to any physical system but were in use during the testing of the collision probability programme. The problem has been solved by the collision probability method, which integrates the angular flux variation explicitly in terms of the E_3 function, and by using an S_n programme SLABBO (Clancy 1969) with weights and ordinates corresponding to a double P_{16} integration of the angular flux. Using these angular directions the objections to the S_n method, based on the possibility of an inadequate representation of the angular flux at high azimuthal angle, can be completely removed. The problem which arises is simply that the use of such a set of ordinates, on a slab problem, with mesh regions 0.6 mean free paths across, requires careful computation of the angular fluxes at high azimuthal angle. This point is discussed in some detail in Section 4 of the recent report of Carlson (1968).

The equation for the angular flux F across a mesh interval can be written

$$\mu \frac{dF}{dx} + \sigma F = S ,$$

with the boundary condition $F(0) = F_{in}$ and the source S assumed flat across the interval.

The solution of this equation is seen to be

$$F(x) = \frac{1}{\sigma} \left[e^{-\sigma x/\mu} \sigma F_{in} + (1 - e^{-\sigma x/\mu}) S \right] .$$

In particular the outward going flux for the mesh interval F_{out} at $x = \Delta$ is simply

$$F_{out} = \frac{1}{\sigma}\left[e^{-\sigma\Delta/\mu}\ \sigma F_{in} + (1 - e^{-\sigma\Delta/\mu})\ S\right],$$

whilst the average angular flux for the interval is

$$\overline{F} = \frac{S}{\sigma} + \frac{\mu}{\sigma\Delta}\left[F_{in} - F_{out}\right] .$$

In some formulations, for example the WDSN code, this form for the outgoing flux is avoided because the exponential is time-consuming. If we use the approximation (correct to second order when $\sigma\Delta/\mu$ is small)

$$e^{-\sigma\Delta/\mu} = \left(1 - \frac{\sigma\Delta}{2\mu}\right)\Big/\left(1 + \frac{\sigma\Delta}{2\mu}\right) ,$$

then the solution becomes simply

$$F_{out} = \frac{2S\Delta}{2\mu + \sigma\Delta} + F_{in}\ \frac{(2\mu - \sigma\Delta)}{2\mu + \sigma\Delta}$$

$$\overline{F} = \frac{1}{2}\left[F_{in} + F_{out}\right] = \frac{S\Delta + \mu F_{in}}{2\mu + \sigma\Delta} .$$

For small $\frac{\sigma\Delta}{\mu}$, the error introduced by this approximation remains tolerable. However, in slab geometry, the need to consider the flux at high azimuthal angles inevitably introduces long path lengths at these high angles and the approximations then become less attractive. In fact the replacement of $e^{-\sigma\Delta/\mu}$ by

$$\left(1 - \frac{\sigma\Delta}{2\mu}\right)\Big/\left(1 + \frac{\sigma\Delta}{2\mu}\right)$$

can lead to negative fluxes in regions with low sources. The code user will often be unaware of this failing, as the scalar flux will usually remain positive despite the appearance of negative angular fluxes at some angles. This problem may not be restricted to slab geometry situations but is at its worst there because angular fluxes at high angles must be considered, and because the angular flux retains its integrity as we pass from one mesh interval to the next.

Codes which recognise the possibility of negative fluxes usually have some 'fix-up' procedure of the type outlined by Carlson (1968). In Table 12 we have presented the fluxes obtained from the collision probability method and the group 1 fluxes obtained by the SLABBO code using the following formulations:

Method 1 – no recognition of negative angular fluxes

Method 2 – negative flux fix-up as proposed by Carlson

Method 3 – the exponential explicitly retained in the equations.

The conclusion to be drawn from these results is clear. Either the collision probability method or the S_n method with the exponential explicitly retained in the formulation should be employed. There can be little justification for retaining the approximations in the angular flux on the grounds of saving computing time when the results produced from such approximations can so easily be in error. One can only speculate on the error in other geometries where path lengths are usually shorter and the angular fluxes more closely interdependent.

6. THE OUTER BOUNDARY CONDITION IN CYLINDRICAL GEOMETRY

Provision has been made in the collision probability programme ICPP for the exact representation of the outer cell boundary, which will be square or hexagonal for a regular array of fuel

rods. Calculations have been previously reported (Doherty 1968) for some natural uranium heavy water lattices and four of these lattices were selected for examination. The lattices were chosen to cover the range of situations of small or large rod in a small or large cell, and are systems 4, 5, 41 and 48 of the above reference (Table 3).

Seven calculations have been performed on each system. In the first three calculations the 15-group structure and the mesh intervals used in the previously reported calculations were retained. The calculations performed were Bonalumi white boundary, numerical integration white boundary, and specularly reflecting boundary. With ample machine time available the physical outer boundary calculations would also have been performed with the full space and energy representation. However, to keep computing time to a realistic level the calculations were performed with five regions in each problem – two in the fuel, one in the can, and two in the moderator. The first three calculations were re-run for each system to determine the effect of the spatial collapse, and the physical outer boundary calculation was also performed for each system. Table 13 contains the full spatial calculation for the first three boundary conditions and Table 14 contains the calculations on the reduced spatial mesh.

The first remark which must be made is that the time involved in the calculations with the physical boundary correctly represented is prohibitive. Routine running of these options cannot be contemplated, though it is useful to have the options available for selectively examining the effect of the boundary condition on the ultimate result. From the results in Table 14 it can be seen that the white boundary condition gives excellent results for systems of this type. When the cell is large the effect of the boundary condition becomes quite insignificant and either can be used. However when the cell is small the difference between the two boundary conditions is appreciable.

Consider the problem as a two-region problem with the central region 1 as the fuel region surrounded by the moderator (region 2). The use of specular reflection leads to an overestimate of P_{11} because every neutron path originating in the fuel again passes through the fuel on each subsequent crossing of the cell. Consequently, P_{12} and P_{21} are underestimated and P_{22} is overestimated. The fission neutrons are produced at high energy in the fuel and since P_{11} is overestimated the fast fission rate is higher than it should be. Thermal neutrons are produced by slowing down in the moderator and since P_{21} is underestimated the thermal fission rate is reduced.

The effect of the specular boundary condition thus depends on the relative importance of the fast and thermal fission rates. In a natural uranium cell the increase in the fast fission rate is the dominant effect and k is increased. By contrast, in enriched cells where the effect was first noticed, the depression of the thermal fission rate dominates and k is decreased.

We note, in passing, that the k values have changed by 3 per cent in going from the full spatial mesh to the five region representation. As the various boundary condition calculations in Table 13 follow the same type of variation as do those of Table 14, we hopefully assert that the conclusion concerning the adequacy of the white boundary condition remains valid for the correct spatial representation.

7. CONCLUSIONS

The previous sections have surveyed some isotropic collision probability solutions to problems more usually solved by some variant of the S_n method. The flat source assumption inherent in the collision probability method is its greatest liability, since the S_n methods have some freedom in the choice of ordinates and weights in determining the level of the source within the group in relation to the boundary angular fluxes. Thus in both cylindrical and spherical geometry the results obtained with different numbers of mesh points vary more rapidly in the collision probability method than in the corresponding S_n calculation. This means simply that the user without a priori knowledge of a particular problem has a better chance of obtaining a good estimate of the parameters of interest with the S_n method. While it would be possible to build into the collision probability calculation a different assumption from that of a flat flux, such a set of routines would lose generality of application with the same rapidity as they effected improvement in particular problems.

In slab geometry the collision probability method is the more attractive, again because the probability of obtaining an acceptable result without a priori knowledge of the problem is higher. In addition the collision probability routines are much simpler in slab geometry than in cylindrical or spherical geometry so that the collision probability scheme is faster than the corresponding S_n solution for a sensible number of regions. For all three geometries the speed of the collision probability method is better for small numbers of mesh intervals and many groups, while the S_n methods are better for large numbers of mesh intervals and few groups.

Finally, the problems tested with the white outer boundary in cylindrical geometry showed that the use of this boundary condition reproduces quite well the results obtained with the physical outer boundary represented without approximation. This result is reassuring because routine calculations using the physical boundary correctly represented are obviously beyond the present computing capabilities of most establishments.

8. ACKNOWLEDGEMENTS

I am indebted to Mr. B. Clancy for illuminating discussion of the S_n method and for the modifications made to his programme SLABBO to facilitate comparison runs in slab geometry. Mr. J. Pollard's assistance in commissioning my programme, and his provision of automatic coupling to the GYMEA programme are gratefully acknowledged.

9. REFERENCES

Argonne Code Center Benchmark Problem Book (1968). – Numerical determination of the space, time, angle or energy distribution of particles in an assembly. ANL-7416.

Askew, J.R. (1967). – Mesh requirements for neutron transport calculations. AEEW-M760.

Askew, J.R. and Brissenden, R.J. (1963). – Some improvements in the discrete ordinate method of B.G. Carlson for solving the neutron transport equation. AEEW-R161.

Askew, J.R., Fayers, F.J. and Kemshell, P.B. (1966). – A general description of the lattice code WIMS. Journal of the BNES 5 (4) : 564.

Beardwood, J.E., Clayton, A.J. and Pull, I.C. (1965). – The solution of the transport equation by collision probability methods. Proc. Conf. on The Application of Computing Methods to Reactor Problems. ANL-7050.

Bonalumi, R. (1961). – Neutron first collision probabilities in reactor physics. Energia Nucleare, 8 (5) : 326.

Carlson, B.G. (1968). – Transport theory: formulations and solutions by finite difference methods. LA-4016.

Carlson, B., Lee, C. and Worlton, J. (1960). – The DSN and TDC neutron transport codes. LAMS-2346.

Clancy, B.E. (1969). – SLABBO – A discrete ordinate transport code in plane geometry with anisotropic scattering. AAEC/TM505.

Doherty, G. (1968). – Theoretical analysis of some heavy water natural uranium lattices. AAEC/TM461.

Doherty, G. (1969a). – Some methods of calculating first flight collision probabilities in slab and cylindrical lattices. AAEC/TM489.

Doherty, G. (1969b). – Solution of the multigroup collision probability equations. AAEC/E197.

Green, C. (1964). – The IBM 7090 programmes PERSEUS, ARIADNE and CERBERUS. AEEW-R390.

Green, C. (1967). – The Winfrith DSN programme, Mark 2. AEEW-R498.

Jonsson, A. (1963). – THESEUS – A one group collision probability routine for annular systems. AEEW-R253.

Leslie, D.C. (1963). – The 'Spectrox' method for thermal spectra in lattice cells. J. Nucl. Energy, 17, 293.

Meneghetti, D. (1961). – Convergence of transport solutions for thin slab cells. ANL-6345.

Newmarch, D. (1960). – Errors due to the cylindrical cell approximation in lattice calculations. AEEW-R34.

Pollard, J.P. and Robinson, G.S. (1969). - 360 GYMEA - A nuclide depletion, space independent, multigroup neutron diffusion, data preparation code (an unpublished extension of the 7040 version, AAEC/E147).

APPENDIX 1

CALCULATION OF COLLISION PROBABILITIES IN SPHERICAL GEOMETRY

The geometry is illustrated in Figure 1. Consider a horizontal plane through the centre of the sphere. Let all neutron paths be vertical (since the problem is rotationally invariant). Let the projection of the neutron path on the horizontal plane be at distance r from the centre. Then $r < r_i$ implies the neutron path cuts the shell i. We define a set of collision probabilities and volumes as follows:

P_{ij}^{k} = probability that aneutron born in region i will collide in region j when the neutron track has projection r with $r_{k-1} < r < r_k$.

V_i^k = the volume of region i associated with tracks where $r_{k-1} < r < r_k$.

The conventionally defined collision probabilities P_{ij} are given by

$$V_i P_{ij} = \underset{k}{\text{Sum}}\ V_i^k P_{ij}^k \quad ,$$

where $$V_j = \underset{k}{\text{Sum}}\ V_i^k \quad .$$

Formulating the problem in this fashion it is not difficult to establish the following results:

$$P_{11}^{1} = 1 - \frac{1}{\Sigma_1 V_1}\int_0^{r_1} 2\pi r\, dr \left[1 - e^{-2\Sigma_1 z_1}\right]$$

$$P_{12}^{1} = \frac{1}{\Sigma_1 V_1}\int_0^{r_1} 2\pi r\, dr \left[1 - e^{-2\Sigma_1 z_1}\right]\left[1 - e^{-\Sigma_2(z_2 - z_1)}\right] \quad ,$$

where $$z_i = \sqrt{r_i^2 - r^2} \quad .$$

Using the notation $z_0 = 0$, $T_i = e^{-\Sigma_i (z_i - z_{i-1})}$,

$$P_{11}^{1} = 1 - \frac{1}{\Sigma_1 V_1}\int_0^{r_1} 2\pi r\, dr \left[1 - T_1^2\right]$$

$$P_{12}^{1} = \frac{1}{\Sigma_1 V_1}\int_0^{r_1} 2\pi r\, dr \left[1 - T_1^2\right]\left[1 - T_2\right]$$

$$P_{1,j}^{1} = \frac{1}{\Sigma_1 V_1}\int_0^{r_1} 2\pi r\, dr \left[1 - T_1^2\right] T_2\, T_3 \ldots \left[T_{j-1}\quad 1 - T_j\right] \quad .$$

As usual P_{ij} for $i > j$ will be obtained by reciprocity so it is necessary to consider only $i \leqslant j$.

$$P_{22}^{1} = 1 - \frac{1}{V_2^1 \Sigma_2}\int_0^{r_1} 2\pi r\, dr \left[1 - T_2\right] + \frac{1}{2V_2^1 \Sigma_2}\int_0^{r_1} 2\pi r\, dr \left[1 - T_2\right] T_1^2 \left[1 - T_2\right]$$

$$P_{23}^{1} = \frac{1}{2V_2^1 \Sigma_2}\int_0^{r_1} 2\pi r\, dr \left[1 - T_2\right]\left[1 + T_1^2 T_2\right]\left[1 - T_3\right]$$

(continued)

$$P_{2,j}^{1} = \frac{1}{2V_2^1\Sigma_2}\int_0^{r_1} 2\pi r\,dr\,\left[1-T_2\right]\,T_3\,T_4\ldots T_{j-1}\left[1-T_j\right]\,\left[1+T_1^2\,T_2\right]$$

$$P_{ii}^{1} = \frac{1}{V_i^1\Sigma_i}\int_0^{r_1} 2\pi r\,dr\,\left[1-T_i\right] + \frac{1}{2V_i^1\Sigma_i}\int_0^{r_1} 2\pi r\,dr\,\left[1-T_i\right]^2 T_1^2\,T_2^2\ldots T_{i-1}^2$$

$$P_{i,i+1}^{1} = \frac{1}{2V_i^1\Sigma_i}\int_0^{r_1} 2\pi r\,dr\,\left[1-T_i\right]\left[1+T_1^2\,T_2^2\ldots T_{i-1}^2\,T_i\right]\left[1-T_{i+1}\right]$$

$$P_{ij}^{1} = \frac{1}{2V_i^1\Sigma_i}\int_0^{r_1} 2\pi r\,dr\,\left[1-T_i\right]T_{i+1}\,T_{i+2}\ldots T_{j-1}\left[1-T_j\right]\left[1+T_1^2\,T_2^2\ldots T_{i-1}^2\,T_i\right]$$

Similar results for P_{ij}^{2}, P_{ij}^{3} . . . P_{ij}^{i} can be written down by noting that in the case of P_{ij}^{k}, region k plays the role of region 1 in the above equations.

Of course, $P_{ij}^{k} = 0$ for $k > i$.

Thus

$$P_{ij}^{k} = \frac{1}{2V_i^k\Sigma_i}\int_{r_{k-1}}^{r_k} 2\pi r\,dr\,\left[1-T_i\right]\left[1+T_k^2\,T_{k+1}^2\ldots T_i^2\right]T_{i+1}\,T_{i+2}\ldots T_{j-1}\left[1-T_j\right] .$$

The r-integration involved in these formulae can be performed using Gauss-Legendre quadrature. It would be possible to derive an approximate method similar to the Bonalumi (1961) method in cylindrical geometry but it does not seem worthwhile, particularly as the collision probability method is mainly for use in few region applications.

The equations have been derived for the free boundary sphere, though it is possible to make the equivalent approximation to the Wigner-Seitz cylindrical approximation and employ the white boundary surface reciprocity relation to cope with spheres embedded in a matrix of other material.

APPENDIX 2

AN INTERPOLATION SCHEME FOR CYLINDRICAL GEOMETRY

A procedure for calculating the collision probabilities in annular systems with square or hexagonal boundaries was presented in a previous report (Doherty 1969a) and is discussed in Section 6 of this report. The possibility of using an interpolation scheme in the resonance absorption programme PEARLS has been discussed, and a scheme was finally implemented in the following way.

We have seen in Section 3 that the Bonalumi approximation with a white boundary is capable of producing most of the desired variation of the collision probabilities with fuel cross section. The moderator cross section is assumed to be constant in the resonance absorption calculation scheme for which this interpolation is designed. It was decided to use the Bonalumi approximation as the basis of the interpolation scheme.

Six equally spaced cross section values per decade were used. The Bonalumi collision probabilities P^1_{ij} were computed for each of the cross section values, as were the 'exact' collision probabilities P^2_{ij} obtained from numerical integration. The following quantities were stored.

$$Q_{ij} = \ln (P^2_{ij} / P^1_{ij}) \quad \text{for } i < j$$

(The collision probabilities P_{ij}, $i \geq j$ can be obtained by reciprocity and summability).

When a set of collision probabilities are required for a fuel cross section σ, the Bonalumi collision probabilities P^1_{ij} are calculated and the factors Q_{ij} are obtained by linear interpolation in the tables. The collision probabilities are then given by

$$P_{ij} = P^1_{ij} \exp(Q_{ij}) .$$

To exhibit the differences in collision probabilities with the various routines available for dealing with annular geometries, Tables 15, 16 and 17 have been prepared. The basic cell is annular with the outer radii, being 1.0, 2.0, 3.0 and 4.0. The cross sections are held constant over each table, being the same for all regions. The tables are labelled as follows:

Case A — Free outer boundary, numerical integration method

Case B — Free outer boundary, Bonalumi approximation

Case C — Specularly reflecting outer boundary, numerical integration

Case D — Isotropically reflecting outer boundary, numerical integration

Case E — Isotropically reflecting outer boundary, Bonalumi approximation

Case F — The outer boundary is a square enclosing the same volume, numerical integration

Case G — The outer boundary is a hexagon enclosing the same volume, numerical integration.

The two main points which can be gleaned from the tables are that the specularly reflecting outer boundary is not a good approximation for either square or hexagonal outer boundaries, and that the Bonalumi routine does give sufficiently close values of the collision probabilities to allow its use in the interpolation scheme described. When the outer boundary is four mean free paths from the centre (in this artificial problem) the effect of the different boundary conditions on the collision probabilities is quite small.

TABLE 1

THE ASKEW PROBLEM SPECIFICATION*

Parameter	Fuel (radius 1.5 cm)	Moderator (radius 12.0 cm)
Group 1		
Σ_a	3.126 E−2	3.605 E−6
$\nu\Sigma_f$	1.908 E−2	0.0
Σ_{11}	3.404 E−1	2.926 E−1
Σ_{12}	1.046 E−5	3.872 E−3
Group 2		
Σ_a	2.136 E−1	1.855 E−4
$\nu\Sigma_f$	2.762 E−1	0.0
Σ_{21}	2.228 E−5	2.178 E−6
Σ_{22}	3.808 E−1	3.838 E−1

* From Askew (1967)

TABLE 2

TWO-GROUP CALCULATIONS

Type	Mesh	Integration	k	Time (sec)			k (Askew)
				C. Prob.	Solve	Total	
WDSN	16	S_4	1.0794		16	47	1.07933
	8	S_4	1.0788		8	30	1.07866
	4	S_4	1.0767		5	26	1.07655
	2	S_4	1.0720		4	18	1.07189
WDSN	16	S_8	1.0808		36	67	1.08079
	8	S_8	1.0802		19	41	1.08011
	4	S_8	1.0781		8	28	
	2	S_8	1.0735		8	22	
WDSN	16	S_{16}	1.0818		262	293	
	8	S_{16}	1.0812		126	148	
	4	S_{16}	1.0791		69	90	
	2	S_{16}	1.0744		45	59	
Bonalumi white boundary collision probability	16		1.0800	3.3	29	32.2	1.0800
	8		1.0831	0.9	5.3	6.2	1.0830
	4		1.0888	0.24	1.7	1.94	1.0887
	2		1.0969	0.06	1.18	1.24	1.0969
	1		1.1030	0.02	1	1.02	1.1030
Integration white boundary collision probability	16	4	1.0830	404	29	433	1.0834
	8	4	1.0850	53	5.3	58.3	
	4	4	1.0898	7.2	1.7	9.9	1.0881
	2	4	1.0975	1	1.18	2.18	
	1	4	1.1034	0.12	1	1.12	1.1034
Integration white boundary collision probability	16	8	1.0830	808	29	837	
	8	8	1.0850	106	5.3	111	
	4	8	1.0898	14.4	1.7	16.1	
	2	8	1.0974	2	1.18	3.18	
	1	8	1.1030	0.24	1	1.24	
Integration white boundary collision probability	16	16	1.0830	1616	29	1645	
	8	16	1.0850	212	5.3	217.3	
	4	16	1.0897	28.8	1.7	30.5	
	2	16	1.0973	4	1.18	5.18	
	1	16	1.1030	0.48	1	1.48	

TABLE 3

TWO-GROUP CALCULATIONS (DIFFERENT DATA)

Type	Mesh	Integration	k	Time (sec)		
				C. Prob.	Solve	Total
WDSN	16	S_4	0.9863			44.9
	8	S_4	0.9855			29.3
	4	S_4	0.9830			19.5
	2	S_4	0.9774			15.8
WDSN	16	S_8	0.9880			65.6
	8	S_8	0.9873			39.3
	4	S_8	0.9849			27.7
	2	S_8	0.9791			19.6
Bonalumi white boundary collision probability	16		0.9871	3.3	32	35.3
	8		0.9906	0.9	10.2	11.1
	4		1.0028	0.24	1.94	2.18
	2		1.0066	0.06	1.24	1.30
	1		1.0138	0.02	1.05	1.07
Integration white boundary collision probability	16	4	0.9908	405	32	437
	8	4	0.9930	53	10.2	63
	4	4	0.9984	7.2	1.94	9.14
	2	4	1.0072	1	1.24	2.24
	1	4	1.0142	0.12	1.05	1.17
Integration white boundary collision probability	16	8	0.9907	810	32	842
	8	8	0.9929	106	10.2	126
	4	8	0.9984	14.4	1.94	16.3
	2	8	1.0071	2	1.24	3.24
	1	8	1.0138	0.24	1.05	1.29

TABLE 4

EIGHT-GROUP CALCULATIONS

Type	Mesh	Integration	k	Time (sec)		
				C. Prob.	Solve	Total
WDSN	16	S_4	1.0741			368
	8	S_4	1.0739			209
	4	S_4	1.0734			119
	2	S_4	1.0735			78
WDSN	16	S_8	1.0746			590
	8	S_8	1.0744			320
	4	S_8	1.0734			191
	2	S_8	*			
Bonalumi white boundary collision probability	16		1.0733	13.3	138	171
	8		1.0745	3.5	26	29.5
	4		1.0769	0.94	7.4	8.3
	2		1.0803	0..26	3.92	4.18
	1		1.0824	0.06	2.8	2.86
Integration white boundary collision probability	16	4	1.0750	1621	138	1759
	8	4	1.0758	212	26	238
	4	4	1.0778	29	7.4	36
	2	4	1.0807	3.88	3.92	7.6
	1	4	1.0823	0.44	2.8	3.24
Integration white boundary collision probability	16	8	1.0750	3242	138	3380
	8	8	1.0758	424	26	450
	4	8	1.0778	58	7.4	65
	2	8	1.0807	7.7	3.9	11.6
	1	8	1.0824	0.84	2.8	3.64

* Method of solution breaks down

TABLE 5

SIXTEEN-GROUP CALCULATIONS

Type	Mesh	Integration	k	Time (sec)		
				C. Prob.	Solve	Total
WDSN	16	S_4	1.0814			1260
	8	S_4	1.0812			690
	4	S_4	1.0809			385
	2	S_4	*			
WDSN	16	S_6	1.0819			1956
	8	S_6	1.0817			1035
	4	S_6	*			
	2	S_6	*			
Bonalumi white boundary collision probability	16		1.0804	26.5	285	312
	8		1.0815	7	56	63
	4		1.0837	1.8	18	20
	2		1.0869	0.50	7.85	8.4
	1		1.0889	0.14	5.1	5.24
Integration white boundary collision probability	16	4	1.0819	3220	285	3505
	8	4	1.0827	424	56	480
	4	4	1.0845	58	18	76
	2	4	1.0872	7.7	7.85	15.6
	1	4	1.0888	0.86	5.1	5.96
Integration white boundary collision probability	16	8	1.0819	6420	285	6705
	8	8	1.0827	842	56	898
	4	8	1.0845	114	18	132
	2	8	1.0873	15.1	7.85	23
	1	8	1.0889	1.58	5.1	6.7

* Method of solution breaks down

TABLE 6

ANNULAR COLLISION PROBABILITIES (BONALUMI)

r_1	r_2	r_3	Σ_1	Σ_2	Σ_3	P_{12}	P_{13}	P_{22}	P_{23}	P_{33}
1.0	2.0	3.0	1.0	1.0	1.0	0.30048	0.07327	0.62391	0.21119	0.61679
1.0	2.0	3.0	1.0	0.5	1.0	0.20230	0.14223	0.44521	0.32497	0.62846
1.0	2.0	3.0	1.0	0.1	1.0	0.05384	0.24837	0.13821	0.53629	0.66181
1.0	2.0	3.0	1.0	0.05	1.0	0.02803	0.26704	0.07512	0.58142	0.67013
1.0	2.0	3.0	1.0	0.01	1.0	0.00580	0.28316	0.01638	0.62383	0.67806
1.0	2.0	3.0	1.0	1.0	1.0	0.30048	0.07327	0.62391	0.21119	0.61679
1.0	1.5	2.5	1.0	1.0	1.0	0.20981	0.13849	0.45671	0.28845	0.62032
1.0	1.1	2.1	1.0	1.0	1.0	0.06318	0.24967	0.16837	0.41686	0.62369
1.0	1.05	2.05	1.0	1.0	1.0	0.03439	0.27252	0.10328	0.44450	0.62398
1.0	1.01	2.01	1.0	1.0	1.0	0.00761	0.29420	0.03064	0.47400	0.62399

TABLE 7

ANNULAR COLLISION PROBABILITIES (EXACT)

r_1	r_2	r_3	Σ_1	Σ_2	Σ_3	P_{12}	P_{13}	P_{22}	P_{23}	P_{33}
1.0	2.0	3.0	1.0	1.0	1.0	0.29880	0.07433	0.62125	0.21026	0.61396
1.0	2.0	3.0	1.0	0.5	1.0	0.20132	0.14310	0.44012	0.32272	0.62606
1.0	2.0	3.0	1.0	0.1	1.0	0.05387	0.24976	0.13394	0.52775	0.66012
1.0	2.0	3.0	1.0	0.05	1.0	0.02809	0.26874	0.07234	0.57118	0.66856
1.0	2.0	3.0	1.0	0.01	1.0	0.00582	0.28524	0.01563	0.61194	0.67661
1.0	2.0	3.0	1.0	1.0	1.0	0.29880	0.07433	0.62125	0.21026	0.61396
1.0	1.5	2.5	1.0	1.0	1.0	0.20644	0.14048	0.45259	0.28938	0.61659
1.0	1.1	2.1	1.0	1.0	1.0	0.06051	0.25047	0.16564	0.42244	0.62013
1.0	1.05	2.05	1.0	1.0	1.0	0.03260	0.27248	0.09991	0.45323	0.62068
1.0	1.01	2.01	1.0	1.0	1.0	0.00707	0.29302	0.02933	0.48616	0.62114

TABLE 8

SELF-COLLISION PROBABILITIES

Integration	P_{11}	P_{22}	P_{33}
4	0.59101	0.62004	0.61306
8	0.59256	0.62107	0.61382
12	0.59276	0.62121	0.61393
16	0.59281	0.62124	0.61396

TABLE 9

SPHERICAL GEOMETRY CALCULATIONS

Mesh	Integration	Time (sec)			k
		C. Prob.	Solve	Total	
10	16	13	10	23	0.987093
20	16	69	32	101	0.993612
30	16	194	89	283	0.994915
40	16	417	186	603	0.995387
50	16	762	342	1104	0.995612
50	4	192	342	534	0.995559
50	8	376	342	718	0.995592
50	12	572	342	914	0.995603
50	16	762	342	1104	0.995612

Quoted best k value = 0.9959702 (ANL-7416)

TABLE 10

FLUXES IN FIRST FIVE MESH POINTS

Mesh	Integration	Flux 1	Flux 2	Flux 3	Flux 4	Flux 5
50	4	1.0	1.000547	0.999082	0.996585	0.993178
50	8	1.0	0.999310	0.997613	0.995031	0.991584
50	12	1.0	0.999172	0.997448	0.994856	0.991405
50	S_{16}	1.0	1.001100	0.999662	0.997262	0.993843

TABLE 11

SLAB PROBLEM SPECIFICATION

Five-Group Data

Material 1 Cross Sections

$\nu\Sigma_f = 1.0$

$\Sigma_{i\to j} = 1.0$

$\Sigma_a = 1.0$

Material 2 Cross Sections

$\nu\Sigma_f = 0$

$\Sigma_{i\to j} = 0.5,\ j \geq i,\ 0$ otherwise

$\Sigma_a = 0.5$

Spatial Data

Free slab problem, 10 regions, mesh interval = 0.1

region 1 contains material 1

regions 2 – 9 contain material 2

region 1 group 1 contains a fixed source 1.0

TABLE 12

GROUP 1 FLUXES

Method	Mesh Point 1	Mesh Point 2	Mesh Point 3	Mesh Point 4	Mesh Point 5
Collision probability	0.10608	0.05207	0.02743	0.01651	0.01047
S_n method 1	0.09427	0.05538	0.02831	0.01643	0.01048
S_n method 2	0.09391	0.05700	0.02910	0.01709	0.01046
S_n method 3	0.10608	0.05207	0.02743	0.01651	0.01046

TABLE 13

RESULTS FOR FULL SPATIAL MESH

System	Calculations	Time (min)	k
4	Bonalumi white	1	1.00335
	integrated white	28	1.00665
	integrated specular	60	1.00696
5	Bonalumi white	1	0.98829
	integrated white	10	0.98804
	integrated specular	22	1.00527
41	Bonalumi white	1	1.01447
	integrated white	10	1.01461
	integrated specular	22	1.02150
48	Bonalumi white	1	0.99487
	integrated white	23	0.99944
	integrated specular	55	0.99994

TABLE 14

RESULTS FOR REDUCED SPATIAL MESH

System	Calculations	Time (min)	k
4	Bonalumi white	0.2	1.04013
	integrated white	1.1	1.04112
	integrated specular	2.6	1.04148
	integrated hexagonal	66	1.04114
5	Bonalumi white	0.2	1.01673
	integrated white	1.1	1.01641
	integrated specular	2.6	1.03356
	integrated hexagonal	300	1.01699
41	Bonalumi white	0.2	1.01739
	integrated white	1.1	1.01724
	integrated specular	2.6	1.02441
	integrated square	195	1.01758
48	Bonalumi white	0.2	1.02924
	integrated white	1.1	1.03020
	integrated specular	2.6	1.03094
	integrated square	75	1.03023

TABLE 15

COLLISION PROBABILITIES WITH $\Sigma = 0.1$ IN ALL REGIONS

$(P_{ij}\ ,\ i = 1, 4\ ;\ j = 1,4)$

Case A				Case B			
0.1149	0.1257	0.09781	0.08216	0.1150	0.1170	0.09176	0.07861
0.04188	0.1539	0.1192	0.08993	0.03901	0.1568	0.1167	0.08647
0.01956	0.07151	0.1626	0.1159	0.01835	0.07001	0.1668	0.1174
0.01174	0.03854	0.08279	0.1656	0.1123	0.3706	0.8384	0.1700

Case C				Case D			
0.2328	0.2801	0.2482	0.2389	0.1471	0.2249	0.2730	0.3550
0.09335	0.3417	0.3004	0.2645	0.07496	0.2558	0.2991	0.3701
0.04964	0.1802	0.4182	0.3519	0.05460	0.1795	0.3532	0.4127
0.03414	0.1134	0.2514	0.6011	0.05071	0.1586	0.2948	0.4958

Case E				Case F			
0.1492	0.2204	0.2717	0.3587	0.1495	0.2285	0.2766	0.3454
0.07347	0.2608	0.2976	0.3682	0.07616	0.2600	0.3027	0.3611
0.05433	0.1786	0.3556	0.4115	0.05533	0.1816	0.3576	0.4055
0.05124	0.1578	0.2939	0.4971	0.04934	0.1584	0.2996	0.5063

Case G			
0.1491	0.2276	0.2753	0.3479
0.07587	0.2592	0.3013	0.3636
0.05506	0.1808	0.3558	0.4084
0.04970	0.1558	0.2917	0.5027

TABLE 16

COLLISION PROBABILITIES WITH $\Sigma = 0.5$ IN ALL REGIONS

$(P_{ij}, i = 1,4; j = 1,4)$

Case A				Case B			
0.4040	0.2974	0.1361	0.07181	0.4040	0.2961	0.1354	0.07209
0.09912	0.4575	0.2299	0.09920	0.09870	0.4632	0.2321	0.09676
0.02722	0.1379	0.4526	0.2052	0.02709	0.1393	0.4575	0.2081
0.01026	0.04252	0.1466	0.4486	0.01030	0.04147	0.1487	0.4530

Case C				Case D			
0.4137	0.3135	0.1602	0.1127	0.4062	0.3056	0.1573	0.1309
0.1045	0.4796	0.2626	0.1532	0.1019	0.4679	0.2566	0.1736
0.03203	0.1576	0.5097	0.3007	0.03147	0.1540	0.4940	0.3205
0.01609	0.06567	0.2148	0.7034	0.01870	0.07442	0.2289	0.6779

Case E				Case F			
0.4064	0.3043	0.1565	0.1328	0.4070	0.3084	0.1626	0.1219
0.1014	0.4729	0.2570	0.1686	0.1028	0.4712	0.2631	0.1629
0.03130	0.1542	0.4958	0.3187	0.03253	0.1579	0.5036	0.3060
0.01898	0.07228	0.2277	0.6811	0.01741	0.06981	0.2186	0.6942

Case G			
0.4068	0.3076	0.1604	0.1251
0.1025	0.4701	0.2601	0.1673
0.03208	0.1561	0.4980	0.3139
0.01787	0.07168	0.2242	0.6863

TABLE 17

COLLISION PROBABILITIES WITH $\Sigma = 1.0$ IN ALL REGIONS

$(P_{ij}, i = 1,4; \quad j = 1,4)$

Case A				Case B			
0.5928	0.2988	0.07433	0.02287	0.5929	0.3005	0.07327	0.02244
0.09960	0.6212	0.2103	0.04794	0.1002	0.6239	0.2112	0.04559
0.01487	0.1262	0.6140	0.1875	0.01465	0.1267	0.6168	0.1887
0.003267	0.02055	0.1340	0.6117	0.003205	0.01954	0.1348	0.6148

Case C				Case D			
0.5931	0.2997	0.07684	0.03031	0.5929	0.2992	0.07596	0.03200
0.09991	0.6228	0.2149	0.06232	0.09972	0.6219	0.2133	0.06506
0.01537	0.1290	0.6261	0.2295	0.01519	0.1280	0.6223	0.2345
0.004331	0.02671	0.1640	0.8050	0.004572	0.02788	0.1675	0.8000

Case E				Case F			
0.5929	0.3008	0.07478	0.03150	0.5930	0.2996	0.07739	0.03008
0.1003	0.6245	0.2138	0.06142	0.09986	0.6266	0.2159	0.06159
0.01496	0.1283	0.6241	0.2326	0.01548	0.1296	0.6293	0.2257
0.004500	0.02632	0.1662	0.8030	0.004297	0.02639	0.1612	0.8081

Case G			
0.5929	0.2994	0.07663	0.03106
0.09980	0.6223	0.2144	0.06349
0.01533	0.1287	0.6247	0.2313
0.004437	0.2721	0.1652	0.8032

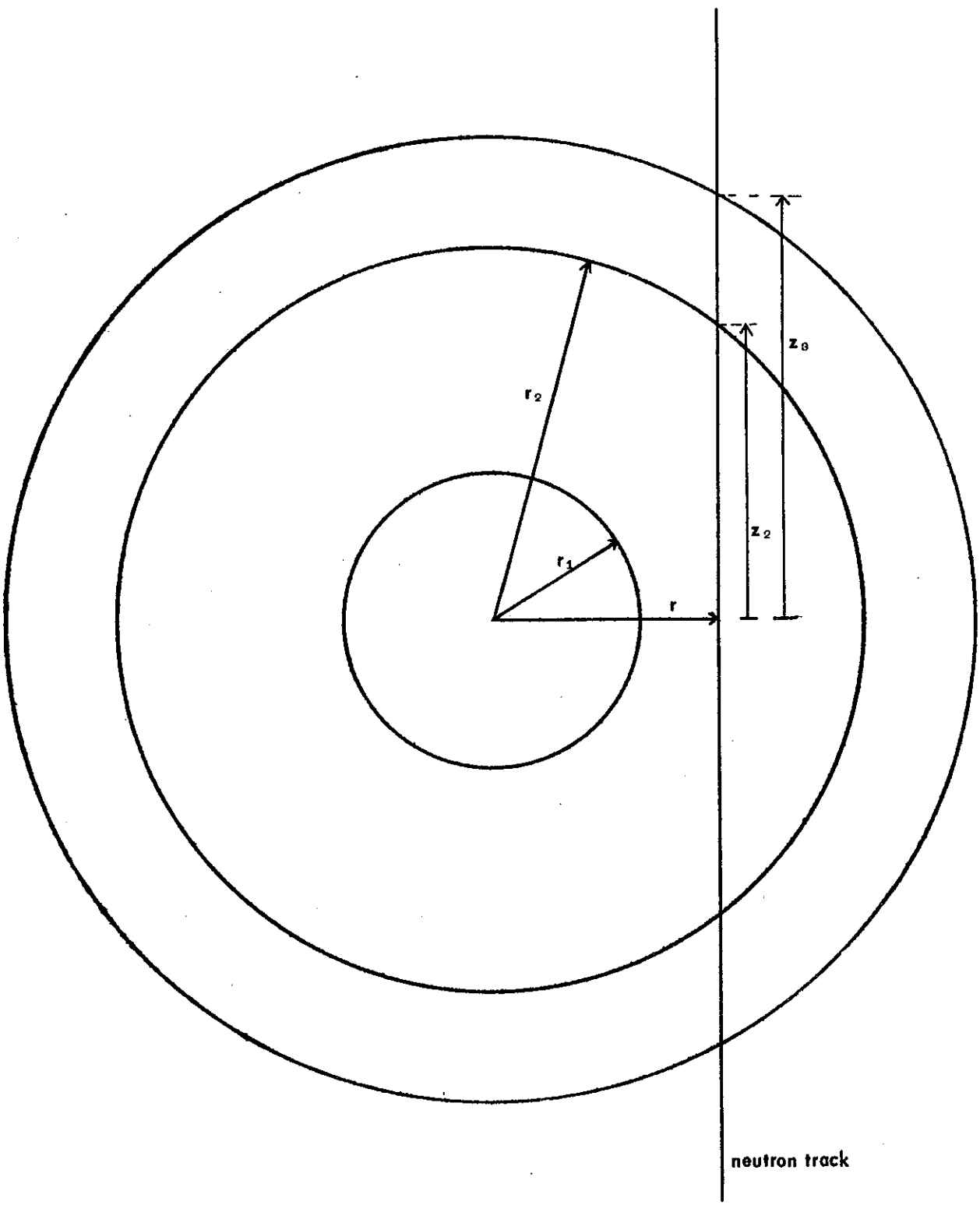

FIGURE 1. SPHERICAL GEOMETRY ILLUSTRATION